Solution Combustion Synthesis of Metal Nanopowders: Copper and Copper/Nickel Alloys

A. Kumar, E. E. Wolf, and A. S. Mukasyan
Chemical and Biomolecular Engineering, University of Notre Dame, IN 46556

DOI 10.1002/aic.12537
Published online February 15, 2011 in Wiley Online Library (wileyonlinelibrary.com).

Based on a general methodology for the preparation of metal–nanopowders by solution combustion synthesis (SCS), the reaction pathways for SCS of pure copper and copper–nickel alloy nanopowders are investigated. It is confirmed that the necessary condition for SCS of metals in a metal-nitrate oxidizer–glycine system is the property of the oxidizer to decompose with formation of HNO_3 species. In this case, for compositions with excess of glycine, a hydrogen reducing atmosphere develops in the reaction front, leading to the formation of reduced metals. The proposed reaction pathways are supported by X-ray diffraction analysis of the quenched samples and DTA–TGA studies of the $Cu(NO_3)_2{\cdot}6H_2O$–glycine and $Ni(NO_3)_2{\cdot}6H_2O/Cu(NO_3)_2{\cdot}6H_2O$–glycine systems. The results show that the formation of Cu_2O and CuO oxide phases takes place at early stages in the reaction front followed by their reduction to pure Cu phase in the postcombustion zones. However, in a Cu–Ni alloy, a fraction of intermetallic Cu–Ni phase appeared directly in the combustion front, whereas the rest of the oxygen-free alloy formed through reduction of oxide phases. © 2011 American Institute of Chemical Engineers *AIChE J,* 57: 3473–3479, 2011

Keywords: combustion synthesis, nanocrystalline materials, Cu nanopowders, Cu–Ni alloy nanopowders

Introduction

Solution combustion synthesis (SCS) on account of its versatility and simplicity, is a unique method for the production of variety of nanomaterials[1–3] in a cost-effective way. SCS is a self-sustained reaction in a homogeneous solution of a metal precursor (oxidizer) and a fuel (e.g., urea, glycine, hydrazine, etc.).[3] The stoichiometric combustion reaction, using a metal nitrate precursor as an oxidizer and glycine as a fuel, can be described by the following widely accepted general scheme:

$$M^{v}(NO_3)_{v}+\left(\frac{5}{9}v\varphi\right)CH_2NH_2COOH+v\frac{5}{4}(\varphi-1)O_2\rightarrow M^{v}O_{\frac{v}{2}}(s)+\left(\frac{10}{9}v\varphi\right)CO_2(g)+\frac{25}{18}\varphi H_2O(g)+v\left(\frac{5\varphi+9}{18}\right)N_2(g) \quad (1)$$

where M^v is a metal with v valence and φ is the fuel/oxidizer ratio. $\varphi = 1$ means that the initial mixture does not require atmospheric oxygen for complete oxidation of the fuel, whereas $\varphi > 1$ (<1) implies fuel-rich (lean) conditions. According to Eq. 1, the final combustion solid product is a metal oxide, and the literature shows that SCS has been primarily used to produce a variety of binary and complex

Correspondence concerning this article should be addressed to E. E. Wolf at ewolf@nd.edu.

nano-oxides.[1–3] No doubt that expanding the capability of the SCS approach for synthesis of other (non-oxides types) compounds, including pure metals and alloys, is an attractive objective. This issue has been partially addressed by some authors[4–6] but, to our knowledge, no detailed reaction pathway has been previously reported.

In our previous work,[7] based on studies of the nickel nitrate–glycine system, a methodology for SCS of pure metal nanopowders was proposed. First, based on literature data and comprehensive studies of this system, it was proposed that the exothermic reaction between NH_3 and HNO_3 species, formed during the decomposition of glycine and nickel nitrate, is the source of the energy required to achieve the self-sustained SCS regime. Second, it was shown that increasing the glycine concentration in the initial solution leads to establishing a hydrogen rich reducing environment in the combustion wave that in turn results in the formation of pure nickel during SCS. Finally, it was concluded that the required conditions for the pure metal formation in the solution combustion systems are:

(i) the oxidizer decomposition with formation of HNO_3 species, and

(ii) the fuel rich ($\varphi > 1$) compositions.

The goal of this article is to apply the proposed reaction pathway to other systems that fits the above requirements, and demonstrate further that by using the proposed methodology, a variety of pure metals and metal alloys can be directly produced by the SCS method. Literature data indicates that another oxidizer, which decomposes with formation of HNO_3 species, is copper nitrate hydrate ($Cu(NO_3)_2{\cdot}6H_2O$).[8] Thus, SCS in two systems $Cu(NO_3)_2{\cdot}6H_2O$–glycine and $Ni(NO_3)_2{\cdot}6H_2O/Cu(NO_3)_2{\cdot}6H_2O$–glycine are investigated here. It is shown that reduced Cu and Cu/Ni alloy nanopowders synthesized under optimized SCS conditions follow the proposed general pathways for pure metal-based synthesis.

Experimental

The following reagents were used as the precursors: copper nitrate hydrate, $Cu(NO_3)_2{\cdot}6H_2O$ (Sigma Aldrich, 99.99%), nickel nitrate hexahydrate, $Ni(NO_3)_2{\cdot}6H_2O$, (Alfa Aesar, 98%), and glycine, CH_2NH_2COOH (Alfa Aesar, 98.5%). The precursor amounts were calculated using the stoichiometric Eq. 1 on the basis of synthesizing 3 g of metal oxide products. These initially solid reagents, were dissolved in the desired ratios in 75 ml deionized water in a 250-ml capacity beaker, and stirred to get a clear homogeneous solution.

The resulting solution was then heated in air on a hot plate (Barnstead Thermolyne, model no: sp 46925 at maximum heating rate setting of 10) until the self-ignition temperature, T_{ig} was reached. A high-speed infrared thermal imaging system (SC6000; FLIR Systems, Boston, MA) was used to monitor the temperature–time history of the process. With FLIR's ThermaCAM Researcher software, thermal images and videos can be captured over several different temperature ranges, which include temperatures as high as 2000°C. Depending on the frame size and temperature range selected; frame rates upward of 15,000 fps are achievable. To obtain data on kinetics of the chemical reaction, a SDT-2960 (TA Instruments, New Castle, DE) was used to conduct simultaneous differential thermal and thermo-gravimetric analysis (DTA-TGA) analysis of the mixtures under the following conditions: argon/air gas flow at 80 cc/min, heating rates 5, 10, and 20 K/min in the temperature range 300–1000 K. To obtain quenched samples, TGA–DTA was stopped at the quenching temperatures.

The as-synthesized powders, as well as quenched samples were characterized by different methods. BET surface area measurements were carried out in a Quantachrome Autosorb-1 unit, using nitrogen as the adsorbent gas. The samples were outgassed at 473 K until the differential pressure fell below 20 μ Hg per min. No other pretreatments were carried out before BET surface area measurements. X-ray diffraction (XRD) measurements were carried out in air in a Scintag X-ray diffractometer with Cu-Kα radiation of wavelength 1.54056 Å. Powder microstructures were analyzed using Field-Emission Hitachi 4500, and Magellan 400 (FEI, scanning electron microscopes [SEM]).

Thermodynamic calculations were performed using the software package "Thermo" to calculate the adiabatic combustion temperature[9] and the equilibrium products under adiabatic conditions. This program is based on optimizing the Gibbs free energy of multiphase and multicomponant systems. It assumes gases to be ideal and condensed phases to be completely immiscible (see details in Ref. 10).

Results and Discussion

$Cu(NO_3)_2{\cdot}6H_2O$–glycine system

Let us first consider the decomposition of glycine and copper nitrate, $Cu(NO_3)_2{\cdot}6H_2O$, as they are precursors for synthesis of copper nano-particles. The TGA plot for glycine decomposition (curve 1) and TGA/DTA data for copper nitrate decomposition in air (curves 2 and 3) are shown on Figure 1a. The TGA graph (curve 2) displays three stages of $Cu(NO_3)_2{\cdot}6H_2O$ decomposition:

(i) before 423 K, a weight loss of ~18 wt %;

(ii) from 423 to 488 K, a weight loss down to ~55% of initial value; and

(iii) from 488 to 543 K, the weight loss down to ~33% of initial value.

It can be also seen that at 543 K, the residual mass reaches ~33% and remains constant up to ~850 K. The corresponding endothermic peaks to these decompositions stages can be observed on the DTA graph (curve 3).

The first stage (<423 K) of mass loss in copper nitrate hydrate is associated with the loss of three moles of hydration water. It was recently shown[8] that the second stage (423–488 K) of Cu nitrate decomposition is attributed to the loss of hydration of water and formation of gaseous HNO_3. The following scheme for this stage of $Cu(NO_3)_2{\cdot}6H_2O$ decomposition in air was proposed[8]

$$2Cu(NO_3)_2{\cdot}3H_2O \rightarrow Cu_2(OH)_3NO_3 + 3H_2O + 3HNO_3 \quad (2)$$

The third stage of mass loss (488–543 K) is related to the decomposition of the remaining nitrate groups and the formation of CuO. The most important result is the presence of HNO_3 during copper nitrate decomposition in the

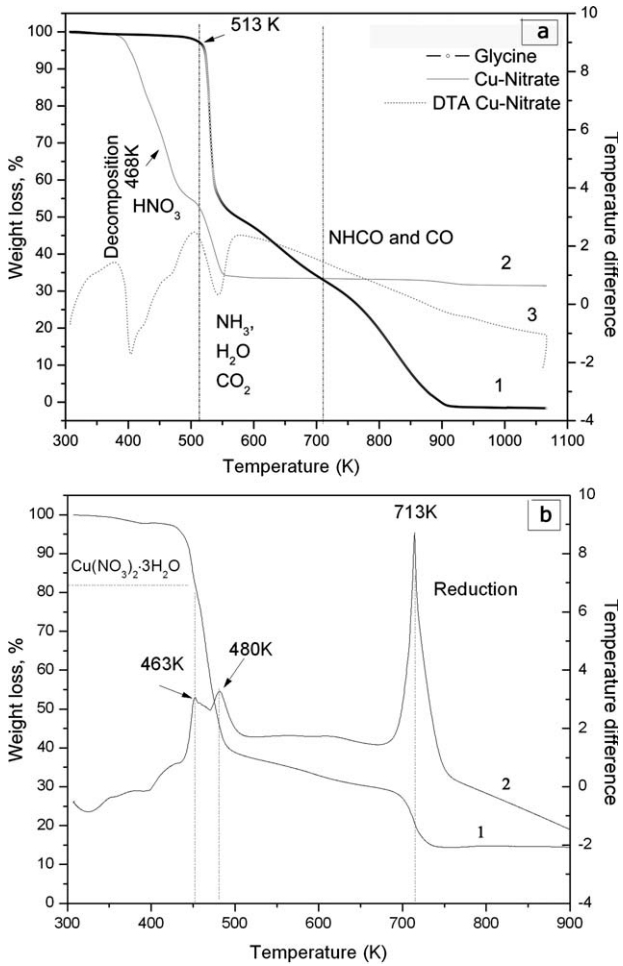

Figure 1. (a) TGA/DTA results for copper nitrate and glycine: (1) TGA glycine, (2) TGA copper nitrate, (3) DTA copper nitrate; (b) DTA–TGA data on reaction in glycine–copper nitrate hexahydrate system: (1) TGA and (2) DTA.

temperature range 423–488 K, which fits the requirements for pure metal formation formulated above.

The decomposition of glycine has been discussed elsewhere[7,11] and can be summarized as follows:

(i) the first stage of weight loss occurs in the temperature range 510–585 K, and the main products of the decomposition are NH_3, H_2O, and CO_2.

(ii) the second stage takes place in the temperature interval 585–730 K and the main products are CO and HNCO.

Now let us consider the copper nitrate and glycine mixture. The overall reaction is assumed to proceed as expressed in Eq. 3:

$$\mathrm{Cu(NO_3)_2}+\frac{10}{9}\varphi\mathrm{CH_2NH_2COOH}+\left[\frac{5}{2}(\varphi-1)\right]\mathrm{O_2}\rightarrow\mathrm{CuO}+\frac{20}{9}\varphi\mathrm{CO_2}+\frac{25}{9}\varphi\mathrm{H_2O}+\left(\frac{5\varphi+9}{9}\right)\mathrm{N_2}\quad(3)$$

The DTA–TGA curves for this reactive mixture, obtained under similar conditions for the data shown in Figure 1a, i.e., air flow and at a heating rate of 20 K/min, are presented in Figure 1b. It can be seen that the first two exothermic peaks are observed in the temperature range 425—500 K, where the major weight loss (~60%) takes place. These temperatures agrees quite well with those corresponding to the region of precursor's decompositions and of the mixture's self-ignition temperature (T_{ig}). As discussed earlier,[7] in this case, the reaction between HNO_3 and NH_3 could be responsible for the vigorous thermal ignition observed in this system at $T_{ig} \sim 450$ K. A much more exothermic peak at $T_{max} = 713$ K, with relatively small reduction of mass is also observed. The equilibrium phases that are formed in the low (425–450 K) and high (700–750 K) temperature stages can be predicted by thermodynamic calculations. These phases can also be experimentally determined by quenching the reactions at different temperatures and by analysis of the resulting solid products by XRD.

Such thermodynamic calculations were performed to understand the effect of $x\mathrm{NH_3}$:$\mathrm{HNO_3}$ ratio in the presence of CuO. Figure 2 shows the adiabatic combustion temperature[9]

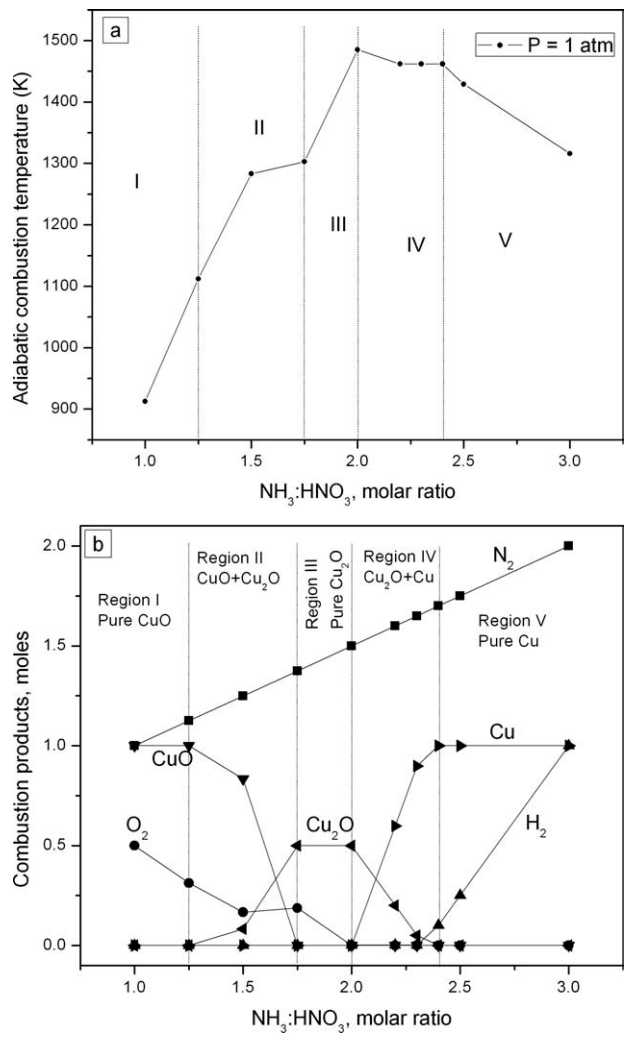

Figure 2. Thermodynamic characteristics of HNO_3: x·NH_3:3·H_2O:CuO system, in molar ratio: (a) adiabatic combustion temperature; (b) equilibrium products.

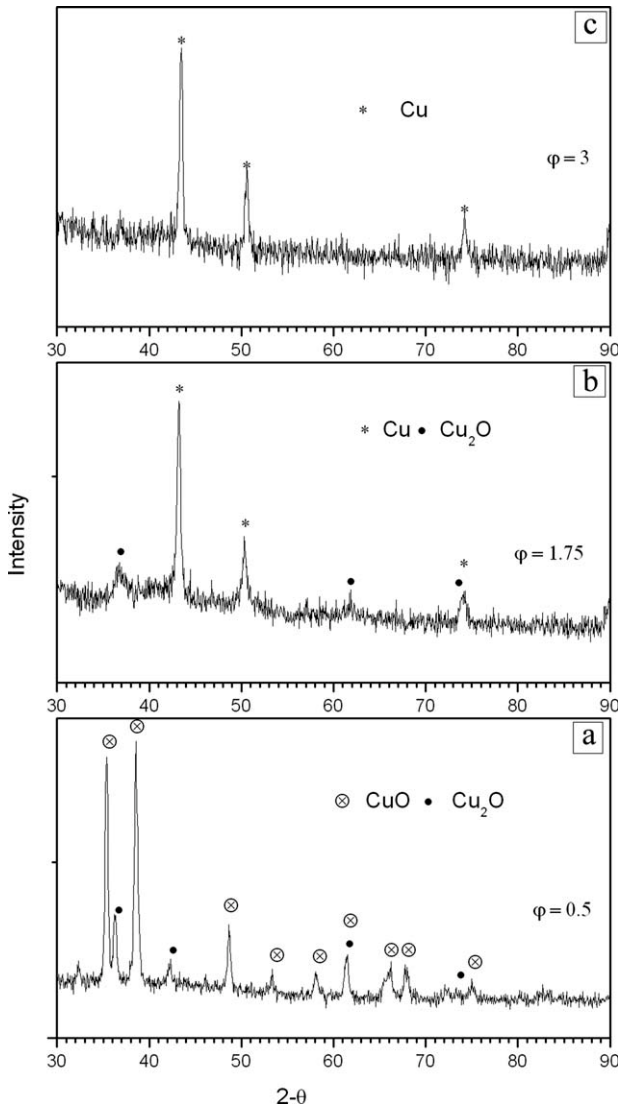

Figure 3. XRD patterns in copper nitrate and glycine system for the products obtained for compositions with (a) $\varphi = 0.5$, (b) $\varphi = 1.75$, and (c) $\varphi = 3$.

(Figure 2a) and the equilibrium products (Figure 2b) in a HNO_3:$x$$NH_3$:3$H_2O$:CuO system, as a function of x, which is proportional to the amount of glycine in the reactive solution. It can be seen that the adiabatic combustion temperature changes from 900 to 1500 K giving a maxima at $x = 2$ as x increases, similar to that for a NiO containing mixture.[7] However in this case, five different regions (Figure 2a) can be outlined based on the predicted equilibrium products (Figure 2b). At relatively small $x < 1.25$ (region I), only pure CuO phase is present in an oxygen rich atmosphere ($0.25 < O_2 < 0.5$). For $1.25 < x < 1.75$ (region II), the presence of Cu_2O along with CuO is predicted in a decreasing oxygen concentration, whereas Cu_2O (region III) is obtained for $1.75 < x < 2$. Reduced Cu along with Cu_2O is present when $2 < x < 2.4$ (region IV) with oxygen disappearing completely while hydrogen starts appearing in this region. For $x > 2.4$ (region V), only pure Cu phase is predicted in a reducing hydrogen atmosphere. From the above, one can conclude

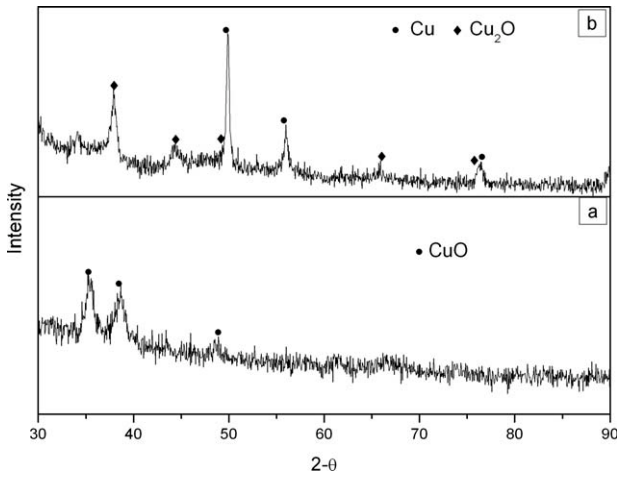

Figure 4. XRD pattern of the products in copper nitrate and glycine system with $\varphi = 1.75$, after first (a) and second (b) combustion waves.

that increasing the ratio of fuel to oxidizer (φ) would lead us to a systematic change in phase from CuO to reduced Cu.

XRD data on phase composition of the final products synthesized by SCS from solutions with different φ ratio are

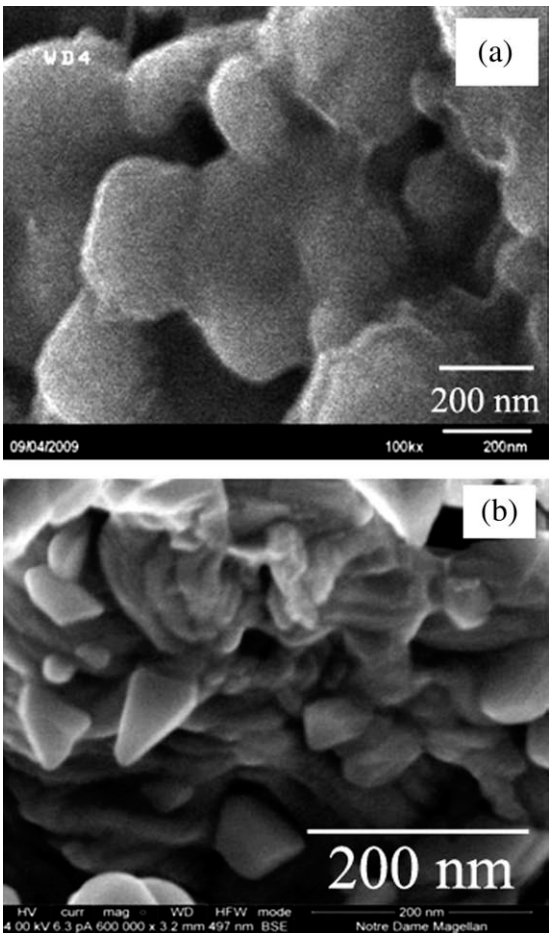

Figure 5. SEM micrographs of as-synthesized pure metals and alloys, $\varphi = 1.75$, conventional SC: (a) Cu and (b) Ni–Cu.

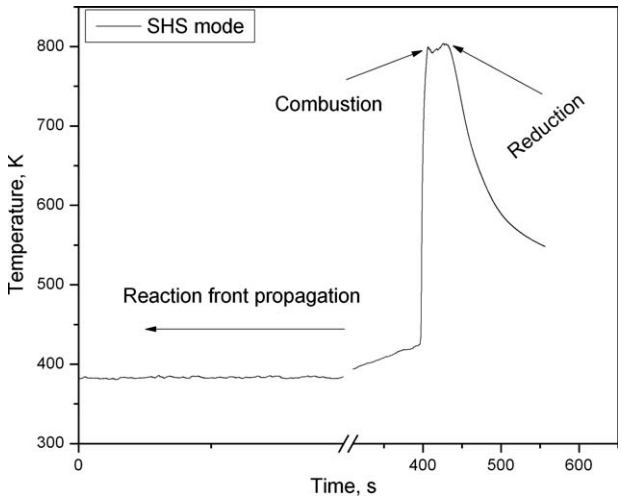

Figure 6. Temperature profiles in $Ni(NO_3)_2{\cdot}6H_2O/Cu(NO_3)_2$ $6H_2O$–glycine system, $\varphi = 1.75$, for SHS mode.

presented in Figure 3. A mixture of CuO and Cu_2O phases are detected for a mixture with low fuel/oxidizer ratio $\varphi = 0.5$ (Figure 3a), whereas Cu and Cu_2O formed for a system with $\varphi = 1.75$ (Figure 3b). Finally, pure Cu is formed during SCS for compositions with a high amount of glycine, $\varphi = 3$ (Figure 3c). These results are in good agreement with the thermodynamic predictions in Figure 2 and suggest the reaction pathway leading to the various phases. To get further insight on the sequence of transformations in the combustion wave, experiments in self-propagating mode were performed.

It was shown that, similar to the nickel-based system,[7] the temperature-time profile of the combustion wave for copper nitrate–glycine solution (not shown in this paper) also involves multiple peaks similar to those observed on the DTA curve (Figure 1b). The latter results suggest the existence of subsequent reduction steps during the combustion process. XRD-analysis results of the quenched sample and

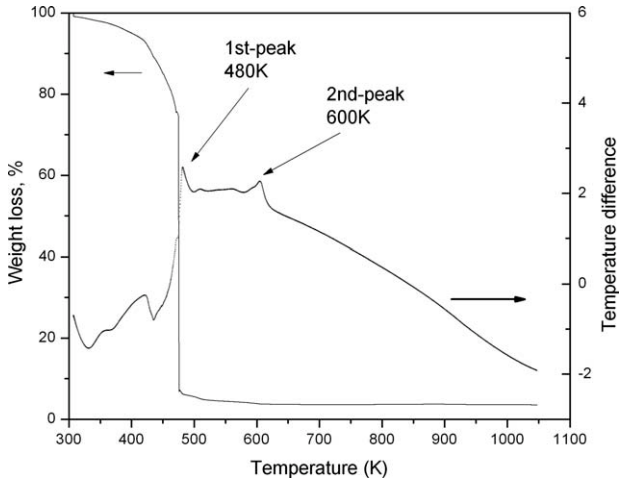

Figure 7. DTA–TGA data on reaction in $Ni(NO_3)_2{\cdot}6H_2O/Cu(NO_3)_2{\cdot}6H_2O$–glycine system, $\varphi = 1.75$.

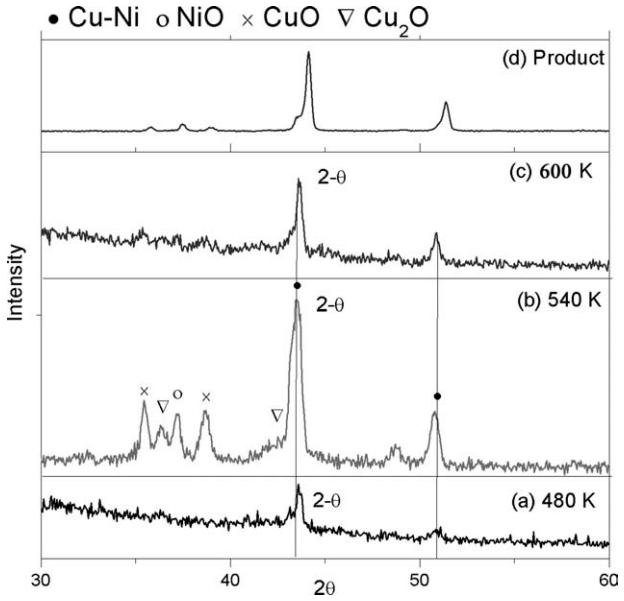

Figure 8. XRD data of samples at different stages of reaction progress in $Ni(NO_3)_2{\cdot}6H_2O/Cu(NO_3)_2$ $6H_2O$–glycine system, $\varphi = 1.75$ (a) 480 K (b) 540 K (c) 600 K (d) final product.

combustion product for a mixture with $\varphi = 1.75$ quenched at ~530 K are shown in Figure 4. It can be seen that the quenched sample is pure CuO (Figure 4a), whereas a mixture of Cu and Cu_2O phases is detected in the product.

Thus, the sequential transformation of CuO → Cu_2O → Cu takes place in the SCS wave. These observations further support the proposed pathway of the combustion reaction in terms of the observed combustion characteristics (self-ignition and maximum combustion temperatures) and the sequence of phase formation in the combustion wave.

Figure 5a shows SEM micrographs of the as-synthesized Cu nanopowders, where particles in 150–200 nm range could be easily seen. Because of the fast propagation of the combustion front, Cu nanoparticles are not as agglomerated as Ni nanoparticles. The surface area of the Cu nanopowder is 15 m^2/g, which is higher relative to an oxide prepared by precipitation and calcination. The next step comes logically from the previous one and is related to the synthesis of complex Cu–Ni metals mixture or alloys, since both Ni and Cu nitrates fit the requirement for pure metal synthesis.

$Ni(NO_3)_2{\cdot}6H_2O/Cu(NO_3)_2{\cdot}6H_2O$–glycine system

A Cu–Ni bimetallic alloy was produced in a similar way to that of reduced Ni and Cu by preparing a homogeneous equimolar mixture of copper and nickel nitrates with glycine in such a way that the ratio φ is 1.75. In this case, after preheating the system to 373 K, the SHS (self propagating high temperature synthesis) regime was attained. The time–temperature profile for the combustion of this system is given in Figure 6. It is similar to that for pure Ni and Cu-based systems, i.e., multiple temperature peaks are detected in the combustion wave, indicating the presence of a sequence of combustion reactions. To understand the mechanism of Cu–

Ni bimetallic formation TGA/DTA results of Cu–Ni system at $\varphi = 1.75$ were obtained. Figure 7 shows that again two temperature peaks can be observed. The first exothermic peak occurs at ~480 K, which corresponds to the maximum decline in sample weight (compare with the position of the first peak for Cu-based system, Figure 1b). This peak is followed by a second peak at ~600 K.

In principle, Cu–Ni bimetallic alloy could be formed by several possible pathways, such as: formation of individual metal oxides first followed by their reduction and formation of the alloy, or formation of ternary Ni–Cu–O phase and its reduction or direct synthesis of Cu–Ni bimetallic phase in the combustion front. To understand the sequence of product development, the reactive mixture was quenched at three intermediate temperatures between 480 and 600 K and the resulting samples were analyzed by XRD. Figure 8a shows that at 480 K, only two lines can be detected that correspond to a Cu–Ni intermetallic phase. As the temperature increases to ~540 K (Figure 8b), the intensity of these two lines increases. However, new lines matching the diffraction patterns for CuO and NiO oxide phases are also present. The intensity of the lines corresponding to the metal oxide peaks decreases at ~600 K (Figure 8c) and the final product (>600 K) involves essentially a pure intermetallic phase (Figure 8d).

These results suggest the following pathway for Cu–Ni phase formation in the SCS wave. During the first stage (first combustion front), while most of the other intermediate products are amorphous, part of a crystalline Cu–Ni phase is formed. This process is followed by crystallization of the NiO and CuO phases as the temperature increases. However, in the second wave, the reduction of the metal oxide occurs with simultaneous formation of intermetallic phase as a result of the reaction between the metals. A SEM micrograph of the as-synthesized Cu–Ni alloy is shown in Figure 5b. In this case, well crystallized domains of ~50 nm with geometric structures appear to protrude from a less well defined matrix. Unfortunately, we cannot determine the individual composition of these domains. The total BET area of this particular alloy was relatively low (2–3 m^2/g) because the combustion wave reached a relatively high temperature resulting in sintering. Although the volume average reaction pathway for the formation of reduced Cu and Cu–Ni alloys confirms the stoichiometric reactions proposed, the reactions at the nanoscale might be more heterogeneous than envisioned in the general pathway.

Concluding Remarks

SCS has been successfully used to produce reduced Ni, Cu metal nanopowders, and their alloys. A reaction pathway has been proposed to describe the phase formation in the combustion front, which is in agreement with the experimental observations for the synthesis of pure Ni, Cu, and Cu–Ni nanopowders.

The proposed reaction pathway can be summarized as follows:

(i) Glycine decomposition starts at about 515 K to yield NH_3.

(ii) Nitrates decomposition occurs in the same temperature range forming HNO_3 and metal oxide.

(iii) NH_3 and HNO_3 react very exothermically sustaining the reaction propagation, while forming hydrogen that further reacts with the metal oxides to yield reduced metals.

(iv) CO and HNCO appear to be the main products in the temperature range 585–730 K and they can reduce the oxides even further at higher temperatures.

The proposed methodology for non-oxide synthesis of nanomaterials by using SCS method can be used for preparation of other pure metals and alloys as well as carbides and nitrides.

Metal nanoparticles are known for their potential application in various fields such as: catalysis, pigments, electronic and magnetic materials, drug delivery, etc. In our laboratory, these materials are being prepared for specific catalytic applications such as: the catalytic hydrogen generation from reforming of bioalcohols.[12,13] Nickel nanoparticles exhibit important catalytic applications because of their activity for various reactions such as steam reforming of methane, steam reforming of ethanol, hydrogenation reactions, hydrocarbon decomposition reactions, etc. Similarly, copper in presence of zinc is known to be active for methanol synthesis and reforming reactions. In our previous work,[14,15] we found that catalysts prepared by SCS were extremely active at low temperatures for hydrogen production from oxidative reforming of methanol, and currently we are applying the SCS approach to synthesize catalysts for other catalytic applications.

Acknowledgments

The authors gratefully acknowledge funding from NSF Grant 0730190 to support this work (to A.K., A.M., and E.E.W.). This work was also partially supported by Notre Dame Integrated Imaging Facility.

Literature Cited

1. Patil KC. *Chemistry of nanocrystalline oxide materials: combustion synthesis, properties and applications*. Singapore: World Scientific Publishing Co. Pte. Ltd, 2008.
2. Aruna ST, Mukasyan AS. Combustion synthesis and nanomaterials. *Curr Opin Solid State Mater Sci*. 2008;12(3-4):44–50.
3. Mukasyan AS, Epstein P, Dinka P. Solution combustion synthesis of nano-materials. *Proc Combust Inst*. 2007;31(2):1789–1795.
4. Choong-Hwan J, Jalota S, Bhaduri SB. Quantitative effects of fuel on the synthesis of Ni/NiO particles using a microwave-induced solution combustion synthesis in air atmosphere. *Mater Lett*. 2005;59:2426–2432.
5. Choong-Hwan J, Hee-Gyoun L, Chan-Joong K, Bhaduri SB. Synthesis of Cu–Ni alloy powder directly from metal salts solution. *J Nanopart Res*. 2003;5:383–388.
6. Erri P, Nader J, Varma A. Controlleing combustion wave propagation for transition metal/alloy/cermet foam synthesis. *Adv Mater*. 2008;20:1243–1245.
7. Kumar A., Wolf EE, Mukasyan AS. Solution combustion synthesis of metal nanopowders part 1: nickel-reaction pathways. *AIChE J*. In press. DOI: 10.1002/aic.12416 (2010).
8. Nikolic R. Physico-chemical characterization of thermal decomposition course in zinc nitrate-copper nitrate hexahydrates. *J Therm Anal Calorim*. 2006;86(2):423–428.
9. Zeldovich YB, Barenblatt GI, Librovich VB, Makhviladze GM. *The Mathematical Theory of Combustion and Explosions*. New York and London: Consultants Bureau, 1985:22–26.
10. Shiryaev AA. Distinctive features of thermodynamic analysis in SHS investigations. *J Eng Phys Thermophys*. 1993;65(4):957–962.
11. Li J, Zhiyong W, Xi Y, Ling H, Yuwen L, Cunxin WJ. Evaluate the pyrolysis pathway of glycine and glycylglycine by TG–FTIR. *J Anal Appl Pyrol*. 2007;80(1):247–253.

12. Sun Y, Cheng J, Hydrolysis of lignocellulosic materials for ethanol production: a review. *Bioresour Technol*. 2002;83:1–11.
13. Öhgren K, Rudolf A, Galbe M, Zacchi G. Fuel ethanol production from steam-pretreated corn stover using SSF at higher dry matter content. *Biomass Bioenergy*. 2006;30:863–869.
14. Schuyten S, Dinka P, Mukasyan AS, Wolf EE. A novel combustion synthesis preparation of CuO/ZnO/ZrO 2/Pd for oxidative hydrogen production from methanol. *Catal Lett*. 2008;121:189–198.
15. Kumar A., Mukasyan AS, Wolf EE. Impregnated layer combustion synthesis method for preparation of multicomponent catalysts for the production of hydrogen from oxidative reforming of methanol. *Appl Catal Gen*. 2010;372:175–183.

Manuscript received Oct. 2, 2010, and revision received Dec. 4, 2010.